Liquid Crystals
Publication details, including instructions for authors and subscription information:
http://www.informaworld.com/smpp/title~content=t713926090

Dynamic simulation of Pi-cell liquid crystal displays

Hongfei Cheng; Hongjin Gao

Online publication date: 06 August 2010

To cite this Article Cheng, Hongfei and Gao, Hongjin(2001) 'Dynamic simulation of Pi-cell liquid crystal displays', Liquid Crystals, 28: 9, 1337 — 1341
To link to this Article: DOI: 10.1080/02678290110058641
URL: http://dx.doi.org/10.1080/02678290110058641

LIQUID CRYSTALS, 2001, VOL. 28, NO. 9, 1337–1341

Dynamic simulation of Pi-cell liquid crystal displays

HONGFEI CHENG* and HONGJIN GAO

Center of Liquid Crystal Technology, Department of Chemistry, Tsinghua University, Beijing 100084, PR China

(*Received 28 November 2000; in final form 15 February 2001; accepted 24 March 2001*)

The dynamics of π-cell liquid crystal displays was studied by detailed computer simulation. The time evolution of the director configuration and the velocity of flow reveals the mechanism of the fast response of π-cells. The effect of pretilt angle on the dynamics of π-cells was also studied.

1. Introduction

Pi-cells were first introduced in the early 1980s as fast light shutters [1]. Their response time is typically a few milliseconds, much faster than most other nematic liquid crystal displays (LCDs). They have also attracted considerable interest for improving the viewing angle of liquid crystal displays because of their self-compensated director configuration [2–12]. Pi-cells are one of the most competitive LCD technologies for future displays.

Although the dynamic response of π-cells is unique among nematic liquid crystal devices, their dynamic properties have not yet been studied by detailed computer simulation. In the dynamic behaviour of liquid crystal displays, the flow of liquid crystal can have an important influence under certain circumstances. For example, the well known optical bounce phenomenon of the twisted nematic (TN) LCD, which occurs after switching off a high applied voltage, is caused by the backflow effect [13, 14].

In this article, the dynamics of π-cells will be studied by detailed computer simulation. The transient property of π-cells is obtained by solving the Ericksen–Leslie hydrodynamic equations. The light transmittance is computed by the Jones matrix method [15].

2. Description of method

The Ericksen–Leslie hydrodynamic equations are

$$\partial_t(\rho v_i) + \partial_j(\rho v_i v_j + p\delta_{i,j} - \sigma^{d}_{ji} - \sigma^{f}_{ji} - \sigma'_{ji}) = 0$$

$$I\,\mathrm{d}^2 n_i/\mathrm{d}t^2 = h_i + h'_i + \gamma n_i$$

where i and j denote x, y, or z components, ρ is the fluid density, v is the fluid velocity, p is the hydrostatic pressure, δ^{d} is the stress tensor from elastic distortion, σ^{f} is the stress tensor induced by electric and magnetic fields, σ' is the viscous stress tensor, h is the molecular field from elastic free energy, h' is the viscous molecular field, I is the rotational inertial density of the fluid, and γ is a Lagrangian multiplier; n is the unit vector of liquid crystal director. In this work, we limited the problem to the one-dimensional case where all the variables depend on z and t. The boundary conditions are that at the substrates, the velocity components vanish and the directors are fixed and time-independent. The explicit expressions for the various quantities can be found in the continuum theory of Ericksen and Leslie [16, 17].

To simulate the dynamics behaviour of the π-cell, we solved the equation of Ericksen–Leslie hydrodynamic theory and then obtained the transient director distribution. The inertial terms in the equation were neglected in the simulation because their influence is very small in comparison with the viscous term. After obtaining the transient director distribution, we calculated the transmittance using the Jones matrix method. Since there are very few measurements of all the viscosity coefficients, here we use the six Leslie viscosity constants for MBBA [14, 18].

3. Results

The parameters used in the simulation are listed in the table. The π-cell has crossed polarizers; the liquid crystal director is at 45° to the crossed polarizers. We

Table. The parameters used in numerical computation.

Cell gap	$d = 5.0\,\mu\mathrm{m}$	$\alpha_1 = 0.0359\ \mathrm{g\,cm^{-1}\,s^{-1}}$
Wavelength	$\lambda = 550.0\,\mathrm{nm}$	$\alpha_2 = -0.4283\ \mathrm{g\,cm^{-1}\,s^{-1}}$
K_{11}	1.24×10^{-7} dyn	$\alpha_3 = -0.0066\ \mathrm{g\,cm^{-1}\,s^{-1}}$
K_{22}	0.6×10^{-7} dyn	$\alpha_4 = 0.4598\ \mathrm{g\,cm^{-1}\,s^{-1}}$
K_{33}	1.71×10^{-7} dyn	$\alpha_5 = 0.2559\ \mathrm{g\,cm^{-1}\,s^{-1}}$
$\varepsilon_{\parallel}$	13.8	$\alpha_6 = \alpha_2 + \alpha_3 + \alpha_5$ (Onsager's relation)
$\varepsilon_{\perp}$	6.6	

*Author for correspondence; e-mail: xzl-dch@mail.tsinghua.edu.cn

Liquid Crystals ISSN 0267-8292 print/ISSN 1366-5855 online © 2001 Taylor & Francis Ltd
http://www.tandf.co.uk/journals
DOI: 10.1080/02678290110058641

calculated the free energies of the bend and splay configurations at different pretilt angles. Figure 1 shows the free energy as a function of applied voltage for the pretilt angle 5°. The voltage at which the bend and splay configurations have equal free energy is defined as the critical voltage V_C. V_C values for pretilt angles 5°, 20° and 35° are 2.5, 1.6 and 1.0 V, respectively. V_C decreases with increasing pretilt angle. In order to obtain the desired π-phase retardation, the transmittance as a function of $d\Delta n$ was calculated at the bias voltage of V_C (d is the cell gap). The first transmittance peak corresponds to the $d\Delta n$ value for π-phase retardation. The $d\Delta n$ values of π-phase retardation for pretilt angles 5°, 20° and 35° are 0.91, 0.99 and 1.36 μm respectively. The dynamic response of π-cells was studied for two main cases; the holding voltage V_H on the π-cell was dropped to either zero or V_C. In principal, a biased voltage is needed to maintain the bend state. To achieve a high switching speed, the applied holding voltage V_H is dropped to zero instead of V_C, and after the material relaxes to the proper state, the bias voltage is applied to maintain the material in the bend configuration.

The configuration evolution after switching off the holding voltage V_H for pretilt angle 5° is shown in figure 2. In figure 2, the applied holding voltage V_H on the π-cell was dropped to zero. The configuration approaches the equilibrium state monotonously; while for a TN cell, the director in the middle of the layer tips over momentarily after switching off a strong applied field [13, 14]. The velocity of flow in the x-direction is shown in figure 3. The x-direction is in the plane of the liquid crystal director of π-cell. The flow pattern is unique in comparison with a TN cell: the velocity has same direction (all positive value) along the z-direction. For any position along the z-direction, the velocity of the

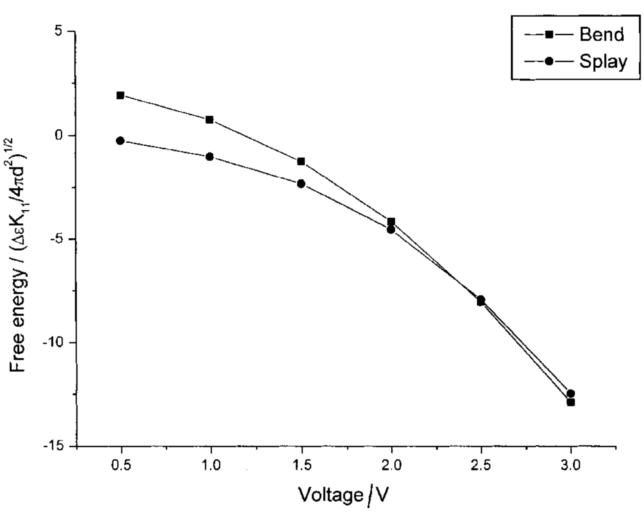

Figure 1. Free energy plotted as a function of voltage for pretilt angle 5°.

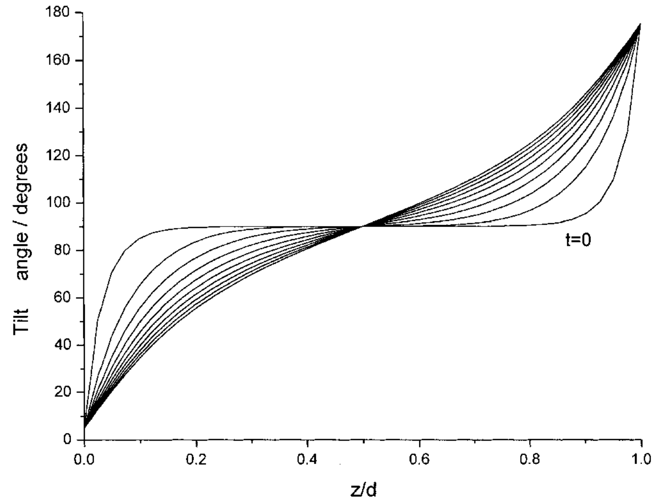

Figure 2. Time-varying configuration after switching off $V_H = 14$ V. The time interval between each pair of neighbouring curves is $\delta t = 0.1$ ms. V_H changes abruptly to 0 V; pretilt angle is 5°.

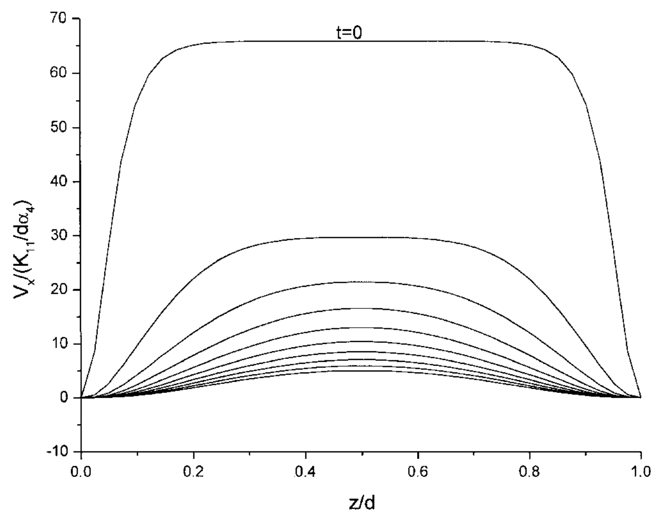

Figure 3. Space and time dependence of flow velocity component V_x after switching off $V_H = 14$ V. The time interval between each pair of neighbouring curves is $\delta t = 0.1$ ms. V_H changes abruptly to 0 V; pretilt angle is 5°.

π-cell approaches zero monotonously without oscillation while a TN cell has a very complex flow velocity pattern after switching off the holding voltage.

To compare the effects of different holding voltages, figure 4 shows the flow velocity for $V_H = 6$ V. The configuration evolution was also studied for different pretilt angles; figure 5 shows the configuration evolution for pretilt angle 35°.

Figures 6 and 7 show the calculated transmittance as a function of time after $V_H = 14$ V is switched off. The applied holding voltage V_H on the π-cell was dropped to

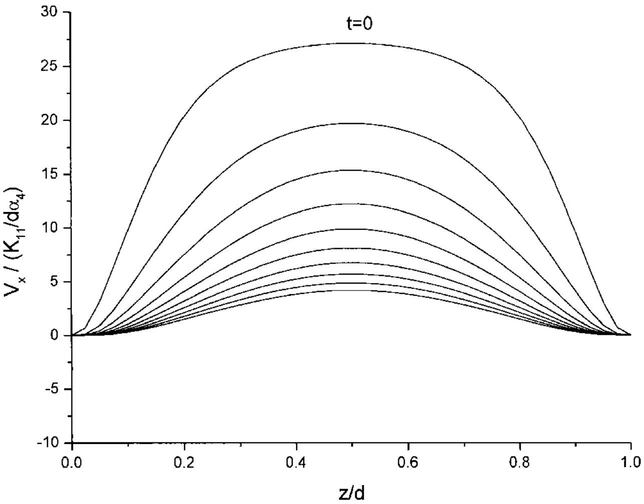

Figure 4. Space and time dependence of flow velocity component V_x after switching off $V_H = 6$ V. The time interval between each pair of neighbouring curves is $\delta t = 0.1$ ms. V_H changes abruptly to 0 V; pretilt angle is 5°.

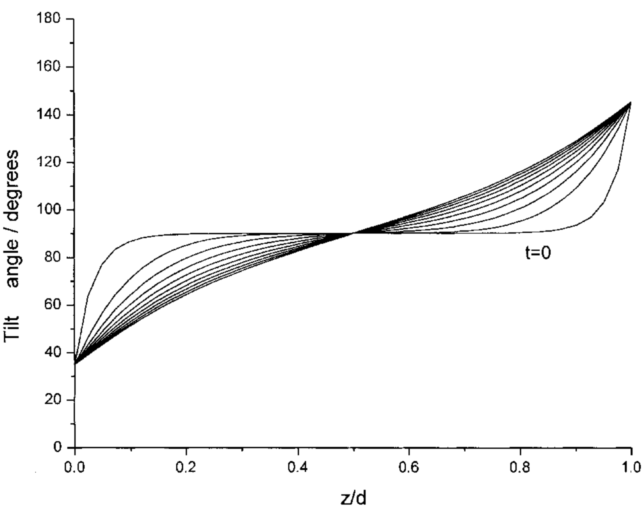

Figure 5. Time-varying configuration after switching off $V_H = 14$ V. The time interval between each pair of neighbouring curves is $\delta t = 0.1$ ms. V_H changes abruptly to 0; pretilt angle is 35°.

V_C and zero, respectively. From figure 6, if the critical voltage V_C is biased at the off state, the response time T_r is faster for the smaller pretilt angle 5° and there is very little difference between pretilt angles 20° and 35°. In figure 7, the response time shows the same tendency, in that T_r increases as the pretilt angle increases. The response time T_r is defined as time required to reach 90% of the maximum transmittance.

Figures 8 and 9 show the calculated transmittance as a function of time after $V_H = 6$ V is switched off. The applied holding voltage V_H on the π-cell was dropped to V_C and zero, respectively. The response time T_r for these

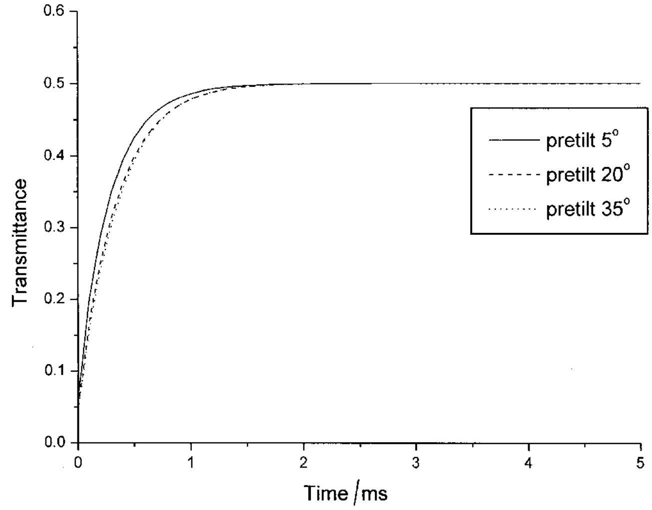

Figure 6. Time-varying transmittance after switching off $V_H = 14$ V; V_H changed abruptly to V_C.

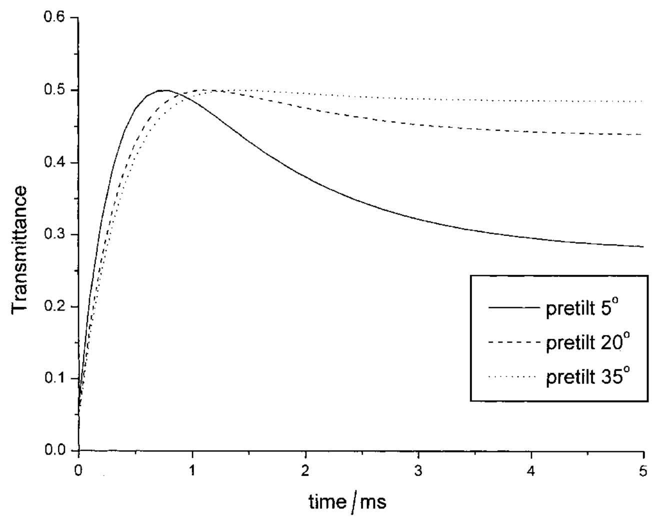

Figure 7. Time-varying transmittance after switching off $V_H = 14$ V; V_H changed abruptly to 0 V.

two conditions has the same tendency in that T_r increases as the pretilt angle increases. But T_r for $V_H = 6$ V is slightly shorter than T_r for $V_H = 14$ V. This is because the holding state at $V_H = 14$ V is farther away from the equilibrium state.

Next we discuss the case when holding voltage V_H is suddenly switched on. Figure 10 shows the configuration evolution for pretilt angle 5° after $V_H = 6$ V is switched on. Figure 11 shows the flow velocity for pretilt angle 5° after $V_H = 6$ V is switched on. Figure 12 shows the transmittance as a function of time. The response time T_f decreases as the pretilt angle increases. T_f actually depends on the magnitude of the holding voltage V_H; it decreases significantly as the V_H increases. The response

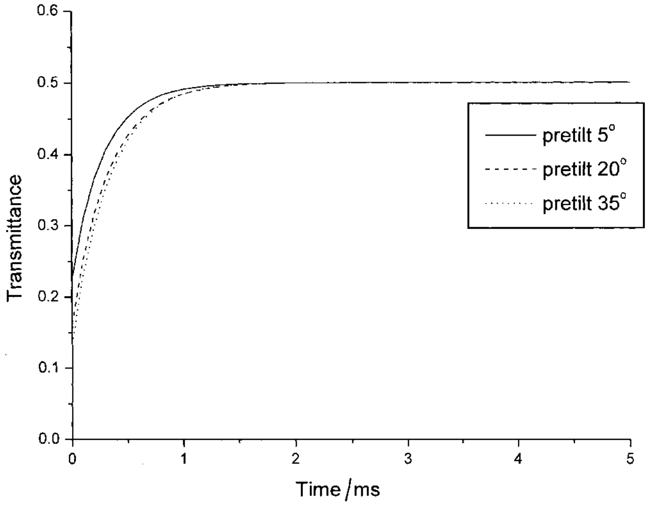

Figure 8. Time-varying transmittance after switching off $V_H = 6$ V; V_H changed abruptly to V_C.

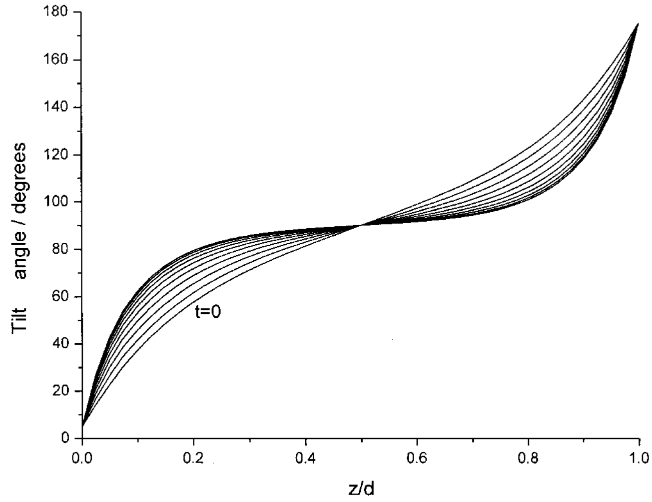

Figure 10. Time-varying configuration after switching on $V_H = 6$ V. The time interval between each pair of neighbouring curves is $\delta t = 0.05$ ms; pretilt angle is 5°.

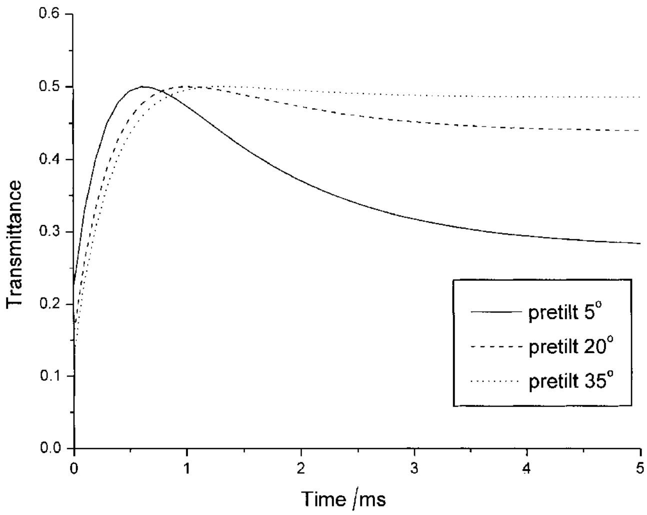

Figure 9. Time-varying transmittance after switching off $V_H = 6$ V; V_H changed abruptly to 0 V.

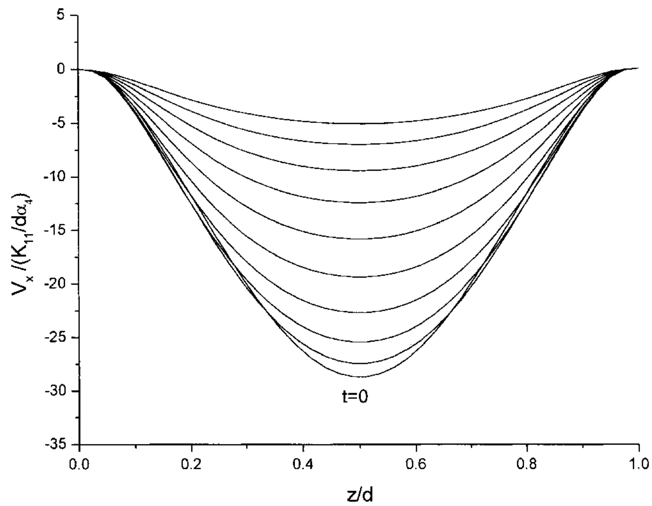

Figure 11. Space and time dependence of flow velocity component V_x after switching on $V_H = 6$ V. The time interval between each pair of neighbouring curves is $\delta t = 0.05$ ms; pretilt angle is 5°.

time T_f is defined as the time required to reach the point where the transmittance is 10% higher than its minimum transmittance.

4. Conclusions

We have investigated the dynamics of π-cells by solving Eriksen–Leslie hydrodynamic equations. This is first time that the dynamic response of π-cells has been studied in detail.

After switching off or on the holding voltage V_H, the tilt angle approaches the equilibrium state monotonously. The velocity of flow across the cell also points in the same direction: all positive or negative. This is where π-cells are distinguished from TN cells. After switching off the holding voltage V_H, the director near the centre of a TN cell tips over; also, the flow velocity of a TN cell across the cell thickness is positive in one region and negative in another.

The effect of pretilt angle on the dynamic response was also studied. The response time T_r increases for a larger pretilt angle after switching off the holding voltage V_H; T_r decreases with larger pretilt angle after switching on the holding voltage V_H.

The magnitude of the holding voltage V_H also has an influence on the dynamic response of π-cells. When V_H is suddenly switched off, the π-cell relaxes to its equilibrium state faster for a smaller V_H value.

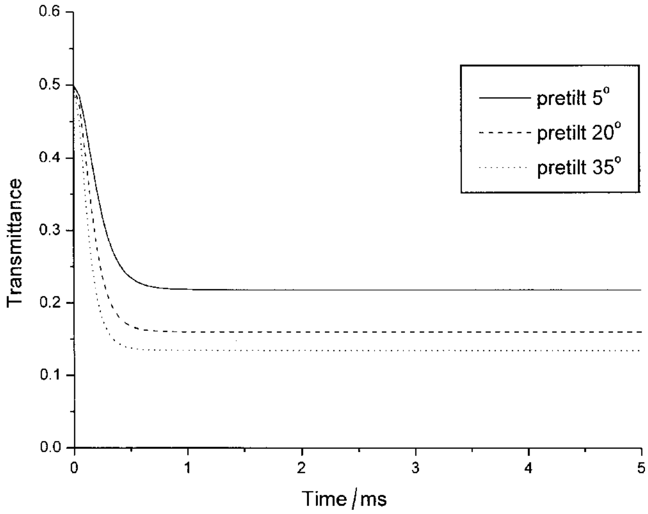

Figure 12. Time-varying transmittance after switching on $V_H = 6$ V.

References

[1] Bos, P. J., and Koehler-Beran, K. R., 1984, *Mol. Cryst. liq. Cryst.*, **113,** 329.
[2] Bos, P. J., and Rahman, J. A., 1993, *SID Dig.*, 273.
[3] Yamaguchi, Y., Miyashita, T., and Uchida, T., 1993, *SID Dig.*, 277.
[4] Mori, H., Itoh, Y., Nishiura, Y., Nakamura, T., and Shinagawa, Y., 1997, *SID Dig.*, 941.
[5] Miyashita, T., Kuo, C. L., Suzuki, M., and Uchida, T., 1995, *SID Dig.*, 797.
[6] Uchida, T., Saitoh, K., Miyashita, T., and Suzuki, M., 1997, *IDRC Dig.*, 37.
[7] Xu, M., Yang, D.-K., Bos, P. J., Jin, X., Harris, F. W., and Cheng, S. Z. D., 1998, *SID Dig.*, 139.
[8] Mori, H., and Bos, P. J., 1998, *SID Dig.*, 830.
[9] Onda, S., Miyashita, T., and Uchida, T., 1998, *Asia Display*, 1055.
[10] Watson, P., Bos, P. J., Gandhi, J., Ji, Y., and Stefanov, M., 1999, *SID Dig.*, 315.
[11] Miyashita, T., Yamaguchi, Y., and Uchida, T., 1995, *Jpn. J. appl. Phys.*, **34,** L177.
[12] Mori, H., and Bos, P. J., 1999, *Jpn. J. appl. Phys.*, **38,** 2837.
[13] Van Doorn, C. Z., 1975, *J. appl. Phys.*, **46,** 3738.
[14] Berreman, D. W., 1975, *J. appl. Phys.*, **46,** 3746.
[15] Jones, R. C., 1942, *J. opt. Soc. Am.*, **32,** 486.
[16] Eriksen, J. L., 1969, *Mol. Cryst. liq. Cryst.*, **7,** 153.
[17] Leslie, F. M., 1966, *Q. J. Mech. appl. Math.*, **19,** 357.
[18] Gäwiler, C., 1971, *Phys. Lett.*, **A36,** 311.